NUCET NUCLEAR ENERGY AND TECHNOLOGY

Nuclear Energy and Technology 10(1): 33–39
DOI 10.3897/nucet.10.122353

Research Article

Towards a uniform description of recombiners performance by a consistent CFD approach with the use of a detailed mechanism of hydrogen oxidation*

Alexander V. Avdeenkov[1], Oleg I. Achakovskii[1], Vladimir V. Ketlerov[1], Sergei L. Soloviev[1], Quang Huong Duong[2]

1 *All-Russian Research Institute for Nuclear Power Plants Operation JSC, 25 Ferganskaya Str., 109507 Moscow, Russia*
2 *IATE MEPhI, 1 Studgorodok, 249039 Obninsk, Kaluga Reg., Russia*

Corresponding author: Alexander V. Avdeenkov (avavdeenkov@vniiaes.ru)

Academic editor: Georgy Tikhomirov ♦ **Received** 30 May 2023 ♦ **Accepted** 2 October 2023 ♦ **Published** 26 March 2024

Citation: Avdeenkov AV, Achakovskii OI, Ketlerov VV, Soloviev SL, Duong QH (2024) Towards a uniform description of recombiners performance by a consistent CFD approach with the use of a detailed mechanism of hydrogen oxidation. Nuclear Energy and Technology 10(1): 33–39. https://doi.org/10.3897/nucet.10.122353

Abstract

For a consistent CFD substantiation of the recombiner performance, a detailed mechanism of hydrogen and oxygen recombination is used. The detailed mechanism of chemical kinetics (multi-step recombination reaction) makes it possible to claim universality, both in the numerical justification of the recombiner performance and in the justification of the flameless recombination threshold and makes it possible to justify the method for optimizing the recombiner to improve its characteristics. The models developed based on this approach were applied to both flat and cylindrical catalytic elements, which are used in FR and RVK recombiners, respectively. As part of the numerical studies, the detailed recombination mechanism was verified, namely the temperature distribution along the catalytic elements was compared and the performance of catalytic elements was compared as well. Good agreement was obtained between the calculated and experimental data. The approach considers not only the mechanism of surface recombination of hydrogen and oxygen on platinum, but also the mechanism of recombination in the gas phase. This makes it possible to calculate the onset of intense combustion outside the catalytic plates, which is a sign of volumetric ignition of the hydrogen-air environment. The concentrations at which such ignition is possible were obtained at different contents of water vapor in the medium. Thus, the proposed approach and the created models make it possible to fully describe the performance of recombiners of distinct designs without the use of additional experimental data, which is extremely necessary when justifying the hydrogen explosion safety of nuclear power plants.

Keywords

recombiner, productivity, chemical kinetics, ignition, multi-step reaction

Introduction

The most widespread practice of emergency hydrogen removal from containments of nuclear power plants is based on using the principle of passive catalytic recombination of hydrogen on various catalytic elements which are part of a passive autocatalytic recombiner (PAR) (Reinecke et al. 2010; IAEA-TECDOC-1661 2011; Avdeenkov et al.

* Russian text published: Izvestiya vuzov. Yadernaya Energetika (ISSN 0204-3327), 2023, n. 4, pp. 61–72.

2018; IAEA International Nuclear Information System (INIS). Catalytic elements are integrated to form catalytic units and large-size assemblies and may have different geometrical forms, including stainless-steel plates coated with a catalytic material based on the Pt/Pd subcomposition (Framatome GmbH), or platinum-blackened cylindrical catalytic elements (LLC ISPC "Russian Energy Technology"). The hydrogen that appears on the catalytic surface in the recombiner's internal volume initiates an exothermic reaction of hydrogen and oxygen recombination into water.

Recombiners of the RVK line (LLC ISPC "Russian Energy Technology") (manufacturer: ZAO INPK RET, Russia) and of the FR line (Framatome GmbH) (manufacturer: AREVA/Siemens) have been certified and are used in Russian nuclear power plants (NPP). The catalytic unit of an RVK-type recombiner includes cylindrical catalytic rods, and FR-type recombiners include plates. The rod or plate number varies among recombiner models and defines the recombiner's overall dimensions and geometry. Experimental data are used to obtain approximating dependences for the recombiner efficiency, that is, for the hydrogen consumption rate (or recombination rate) (Bachellerie et al. 2003; Tarasov et al. 2017; Avdeenkov et al. 2018; Avdeenkov et al. 2022). The obtained dependences are purely empirical and can hardly be used to calculate the recombiner efficiency beyond the experiment scope, since the recombiner performance is highly dependent on the rate of the hydrogen-air mixture delivery into the recombiner (Reinecke et al. 2005; Avdeenkov et al. 2018; Malakhov et al. 2020).

The empirical correlations obtained make it possible to determine the specific efficiency of catalytic elements (the efficiency per unit of the catalyst surface area). Fig. 1 shows the dependences of specific efficiency for two recombiner types, namely the RVK and FR types, on the inlet hydrogen volume fraction, which are rather close taking into account the potential errors in obtaining empirical correlations (deviations of up to ~20%). This indicates that the absolute efficiency is defined mostly by the catalytic surface area, at least with relatively low hydrogen concentrations (<8 vol. %). With higher concentrations of hydrogen, the situation is not so straightforward and may depend on the geometry of catalytic units. When the concentration is low, hydrogen recombination takes place on the catalyst surface, and the area of these surfaces is what mostly defines the PAR efficiency, while the geometry of catalytic elements (plates or rods and their positions against each other) plays a secondary role. With a higher concentration, recombination takes place both on the catalyst surface and in the gas volume inside the recombiner volume, and the geometry of the catalytic unit may therefore have effect on the "ignition concentration" of the air-hydrogen mixture.

As shown by numerical simulations of emergency modes with a major hydrogen yield, the conditions of the environment in the recombiner region are far from those for which the above empirical correlations were obtained.

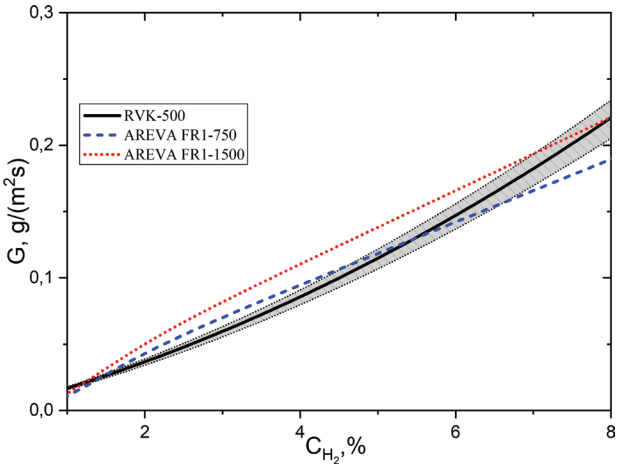

Figure 1. Comparison of specific efficiencies for RVK- and FR-type PARs as a function of hydrogen volume concentration.

Most cases require considering transients since the supply rate and concentration of hydrogen are fast to change and the rate of the air-hydrogen mixture delivery into the recombiner have major effect on its efficiency.

Consequently, large-scale numerical or, moreover, experimental justification for the recombiner operation in all possible non-steady-state and transient modes is challenging, and the essential step in justification of hydrogen safety is to build a working recombiner model of any scale and for any environmental conditions. The approach under development uses a detailed chemical kinetics mechanism (a multistep recombination reaction), which makes it possible to claim the universality of the recombiner operation description due to using known rates of chemical reactions both on the recombiner surface and in the gas phase.

Verification of the detailed recombination mechanism with use of the STAR CCM+ CFD-code

This section presents a computational analysis for recombination of hydrogen using the STAR CCM+ code (Siemens STAR CCM+ CFD software). The conjugate approach to solving thermal hydraulics and chemical kinetics problems was demonstrated successfully in (Baggemann et al. 2013; Reinecke et al. 2013; Malakhov et al. 2020; Avdeenkov et al. 2022), which present its key details, and was used for the calculations discussed in the paper. The surface chemical reaction for platinum-based catalytic oxidation of hydrogen (Appel et al. 2002) includes 12 reactions. The chemical kinetics of the hydrogen burning gas phase in air (Chemical-Kinetic Mechanisms for Combustion Applications) includes 21 reactions. The approach has been numerically implemented and tested based on experimental data both for the FR-type catalyst (rectangular plates, REKO-3 experiments (Reinecke et al. 2005; Avdeenkov et al. 2018), and for the RVK-type catalyst (cylindrical rods, HYSA experiments (Malakhov et al. 2020).

Plate-type FR catalyst

Four catalytic plates (catalyst-coated stainless steel) in the REKO-3 facility are installed in parallel forming vertical rectangular flow channels. Such design represents a section of the FR-type recombiner (Reinecke et al. 2005). The calculations were conducted in a two-dimensional statement with (Reinecke et al. 2005, 2013) taken as the example, that is, the influence of boundary effects due to the finiteness of the plate width is neglected.

Fig. 2a shows the experimental temperature profiles and the calculation results obtained for different inlet concentrations of hydrogen with the air-hydrogen mixture flow rate velocity being v = 0.8 m/s. Fig. 2b shows the experimental profiles of hydrogen concentration and the calculation results for different values of the inlet average air-hydrogen mixture velocity. The calculated hydrogen temperature and concentration profiles are shown for the central channel. The obtained agreement with experimental data is good enough, except for the results for a very low concentration of 0.5 vol. %. It should be noted that the calculations are rather sensitive to the geometry details, e.g. a small distance between two plates (about 1 mm) changes the calculated temperature profiles by tens of degrees. Such sensitivity shall be probably taken into account in processing experimental data.

Cylindrical RVK catalyst

For the numerical testing of the approach using cylindrical (rod shaped) RVK-type catalysts, we used some of the experimental data given in (Malakhov et al. 2020), where the details and parameters of the experiment are discussed.

The flow channel of the test bench is a vertical rectangular box (cross-section area 45.5 mm × 242 mm) which accommodates the RVK recombiner frame with 14 catalytic rods (Fig. 3). A turbulator, a plate with holes, is installed in the lower part of the box, which significantly homogenizes the mixture and slows down its speed. The surface temperatures are measured using an infrared camera (see (Malakhov et al. 2020) for more details). To measure hydrogen concentration, the sensors are fixed in two places - under and above the catalyst section.

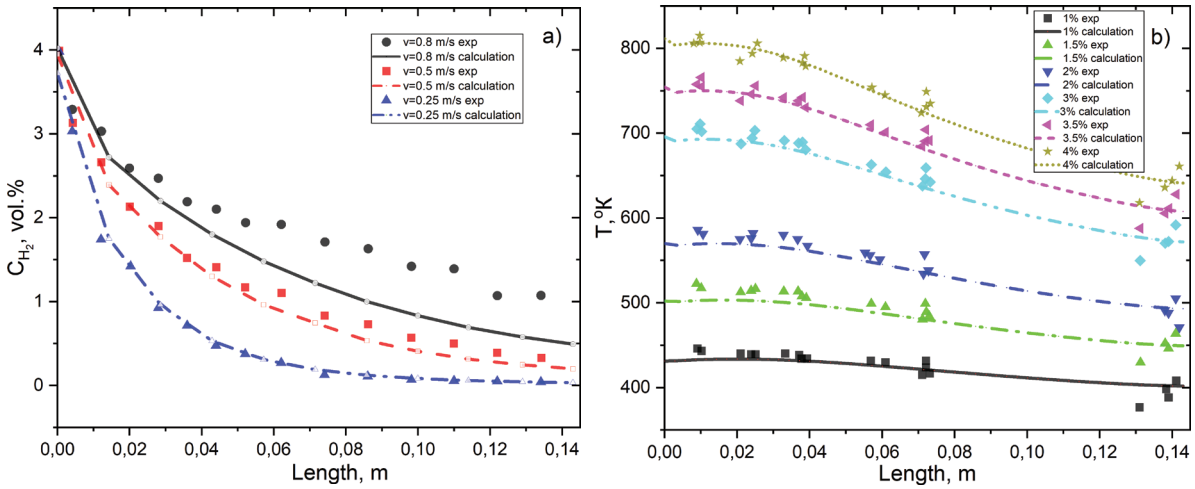

Figure 2. Hydrogen concentration profiles (**a**) and temperature profiles (**b**): REKO-3 experimental data (Reinecke et al. 2005) and STAR CCM+ calculation results (Avdeenkov et al. 2022).

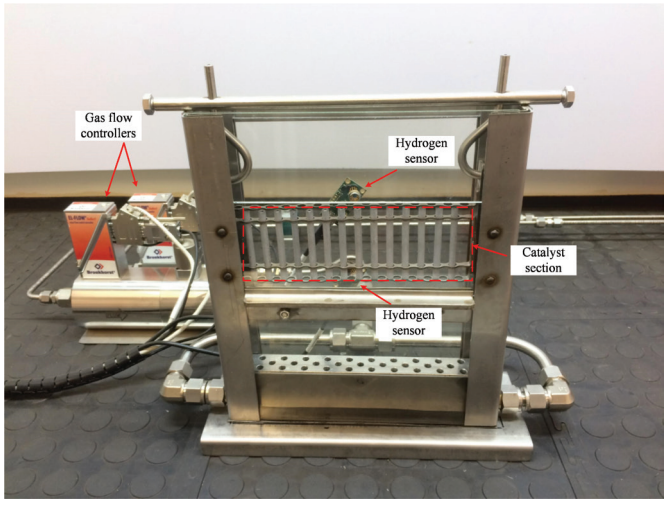

Figure 3. Experimental setup including a catalyst section, hydrogen sensors and gas flow controllers (Malakhov et al. 2020).

Fig. 4 shows representative calculation results for the hydrogen temperature field and relative fraction distribution. The calculation results are shown for the hydrogen concentration of 4 vol. %. The calculations clearly show a higher heating of the central rods. Much of the hydrogen escapes past the catalytic frame, left and right of it, being further mixed with the hydrogen that has passed through but has not had enough time to recombine in the catalytic frame. The mixture flow obtained by using the vortex generator makes the rate of its delivery to the catalyst small.

Fig. 5a shows the experimental temperature profiles for all 14 rods and the calculation results for seven rods on one side of the channel, since the numerical model is symmetrical relative to the plane between rods 7 and 8, while, however, no full symmetry of the temperature profiles have been revealed for symmetrically positioned rods. All temperature profiles have two minimums each, matching the positions of the stainless-steel frame parts which retain the rods in their vertical position. These stainless-steel components evidently have effect on the temperature values of the rod catalytic surfaces at the respective rod positions (the rods are not held rigidly by the frame and play slightly); and, as such, the temperatures in the region of the steel frame components extracted in the course of the experiment are the steel temperatures rather than the rod catalytic surface temperatures. Computationally, this leads to extra difficulties in terms of the simulation accuracy and, specifically, in the accuracy of reproducing the experimental results in the vicinity of the frame components. It can be seen when comparing the experimental results and the calculations that the greatest differences are for the ends of the rods on the frame periphery.

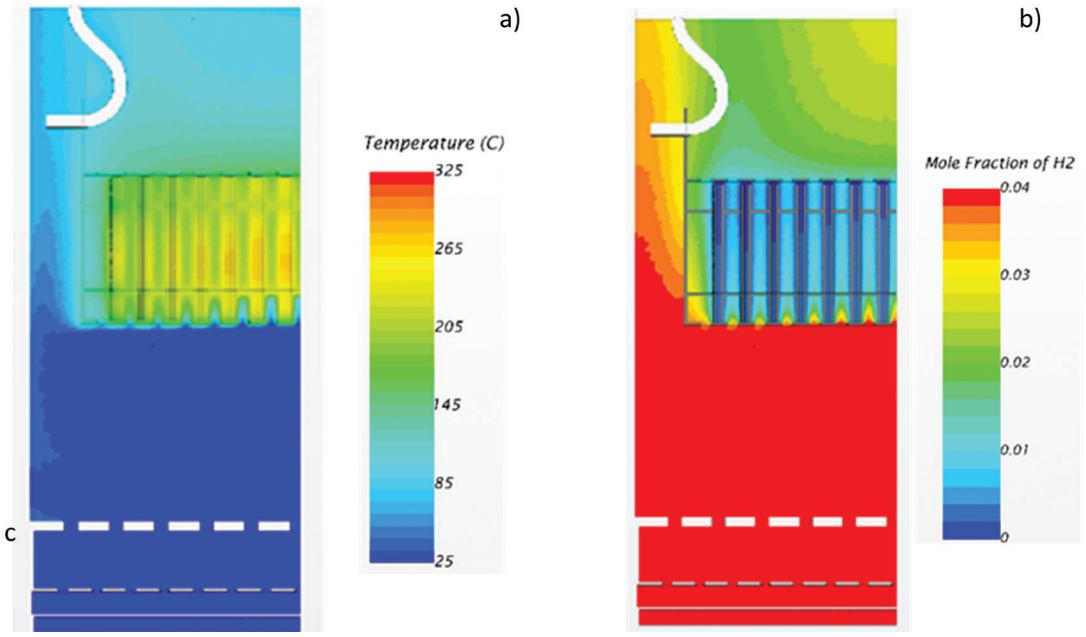

Figure 4. Temperature field (**a**) and mole-fraction hydrogen distribution field (**b**) with 4 vol. % of hydrogen (inlet).

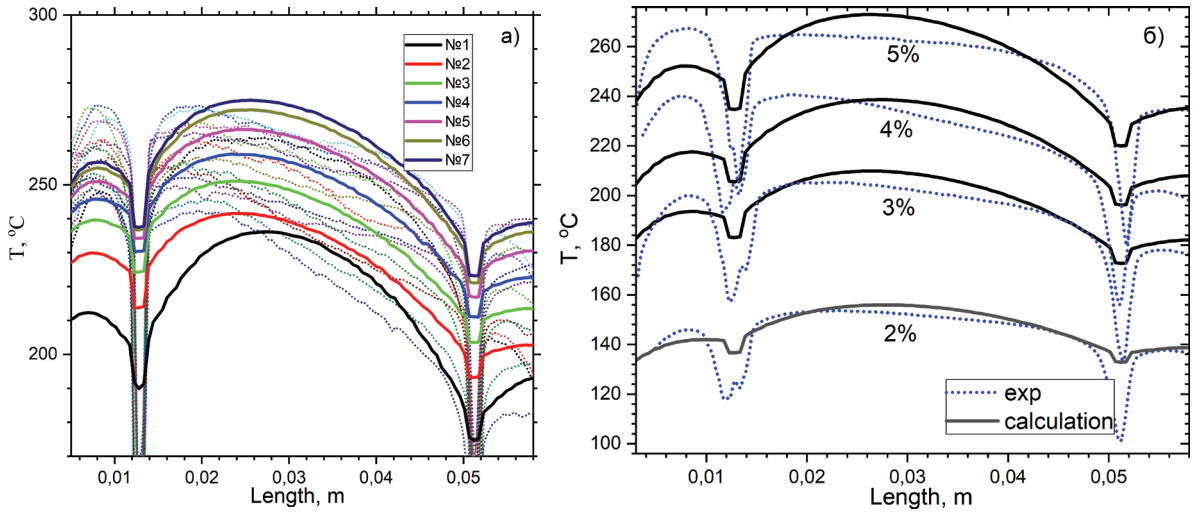

Figure 5. Temperature profiles: HYSA experimental data (Malakhov et al. 2020) (dashed lines) and STAR CCM+ calculation results (Avdeenkov et al. 2022) (solid lines for seven rods) with inlet hydrogen concentration of 4 vol. % (**a**). Calculated and experimental temperature profiles with different inlet hydrogen concentrations averaged over all 14 rods (**b**).

Fig. 5b shows experimental and calculated temperature profiles averaged over all 14 rods. Table 1 shows the experimental and calculated values of hydrogen concentration at the location of the hydrogen sensor above the catalytic frame. Considering the complexity of the experiment and the calculated sensitivity to the details of the bench geometry, a very good agreement was obtained. Thus, the calculations demonstrate the successful application of the method using a detailed hydrogen recombination mechanism based on the available experimental data both for the plate-type FR recombiner and for the rod-type RVK recombiner. This approach will be used further to build a full-scale CFD model of the recombiner and to evaluate the scalability of its efficiency.

Table 1. Hydrogen concentration at the top point above rods

Inlet concentration of H_2, %	Experiment, %	Calculation, %
2	1.01	0.90
3	1.42	1.32
4	1.82	1.73
5	2.14	2.14

Calculation of the flameless recombination limit

Recombination of hydrogen and oxygen on a catalytic surface (or, more precisely, their recombination rate) defines the recombiner efficiency in general and is one of the main characteristics of the recombiner performance but is not its only essential one. The consistent approach includes not only the computational justification for the efficiency but also for another important recombiner characteristic, namely, determination of the flameless recombination limit (or ignition limit). This requires taking into account the detailed mechanism of recombination not only on the catalyst surface but also in the gas phase inside the recombiner volume.

To quantify the flameless recombination limit, a methodology was proposed in (Meynet and Bentaib 2012) for calculating the hydrogen recombination on the catalyst and in the gas phase between the catalytic plates. The hydrogen flameless recombination limit (or the ignition limit) is determined from an abrupt increase in the energy release rate in the gas volume as the energy release rate decreases simultaneously in the surface catalytic layer. It was shown for the plate-type FR recombiner that the noticeable contribution of bulk combustion starts when concentrations are somewhat larger than 6 vol. % in a dry gas mixture.

The calculation results were considered further with the following initial data for the air-hydrogen mixture: inlet velocities of 0.2, 0.8 and 2 m/s without water vapor with the initial mixture temperature of 300 K, and with 45 vol. % of vapor and the initial mixture temperature of 373 K. The initial data in use are rather typical of the recombiner operation and were used in the REKO-3 experiment (Reinecke et al. 2013) but for hydrogen concentrations other than having caused the mixture ignition. All of the calculations presented as part of the study are based on the procedure described in a 2D symmetrical statement for a simplified geometry that contains two FR-type catalytic plates, due to which the recombination rates are given in kg/s/m, that is, per unit of the plate width.

Figs 6–8 present calculations for the recombination rate with different inlet velocities of the gas mixture. Since energy is released due to the recombination, it is more convenient to compare exactly the recombination rate on the surface and in the space (volume) between catalytic plates. The calculation results for the inlet velocity of 0.8 m/s show clearly that there is a sharp increase in the volume recombination growth observed starting approximately with a hydrogen concentration of 6 vol. %. With a vapor concentration of 45 vol. %, the volume recombination does not start earlier than with a hydrogen concentration of 8 vol. %.

Fig. 7 presents the results for the recombination rate with the inlet gas mixture velocity of 2 m/s. On the whole, the calculations have produced similar results at the inlet mixture velocity of 0.8 m/s for the hydrogen concentration starting from which the volumetric ignition of the mixture occurs (ignition), although at slightly lower values of hydrogen concentration. An increase in the gas mixture velocity obviously leads to an increase in the recombination rate,

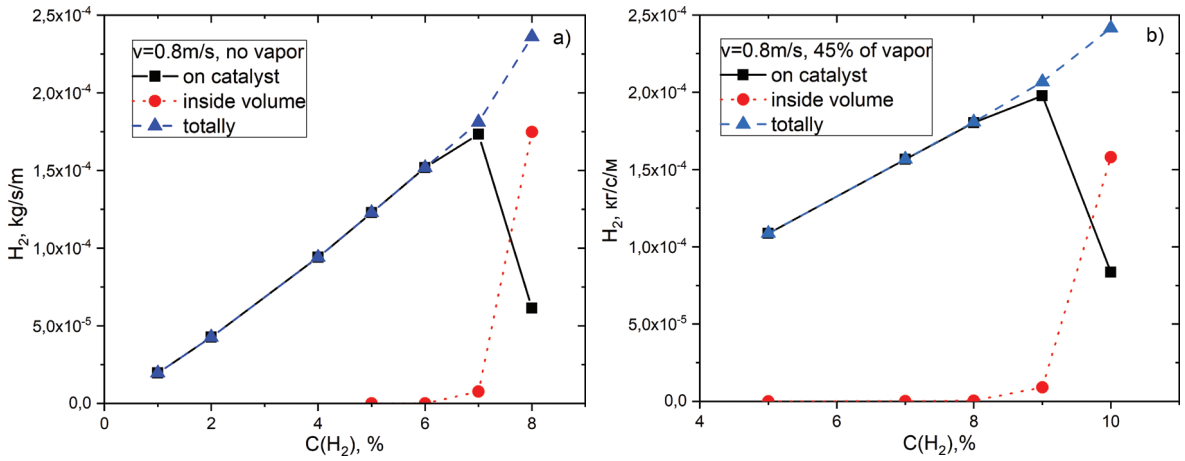

Figure 6. Hydrogen recombination rate as a function of hydrogen concentration: without vapor (**a**) and with a vapor concentration of 45 vol. % (**b**) at the initial time point (inlet flow velocity 0.8 is m/s).

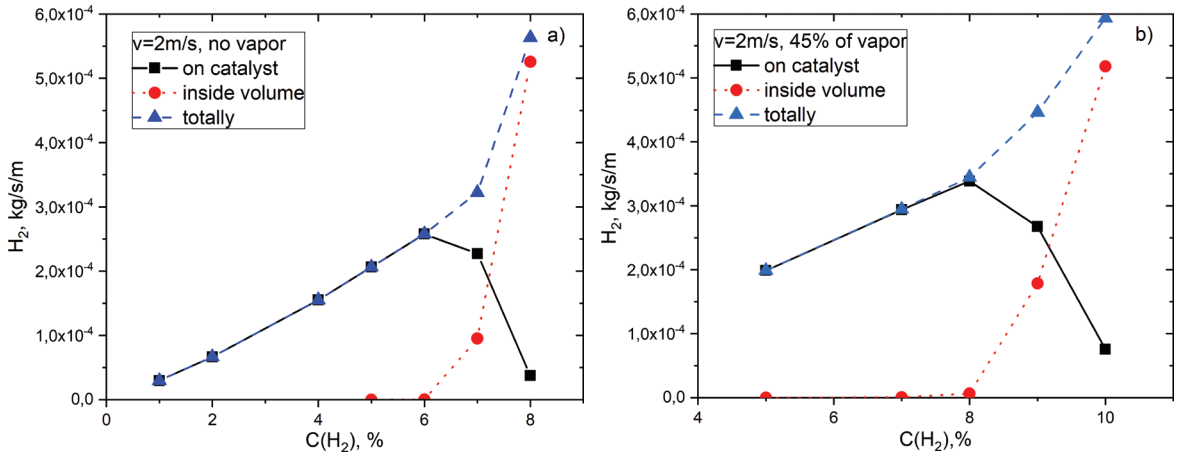

Figure 7. Hydrogen recombination rate as a function of hydrogen concentration, without vapor (**a**) and with a vapor concentration of 45 vol. % (**b**) at the initial time point (inlet flow velocity is 2 m/s).

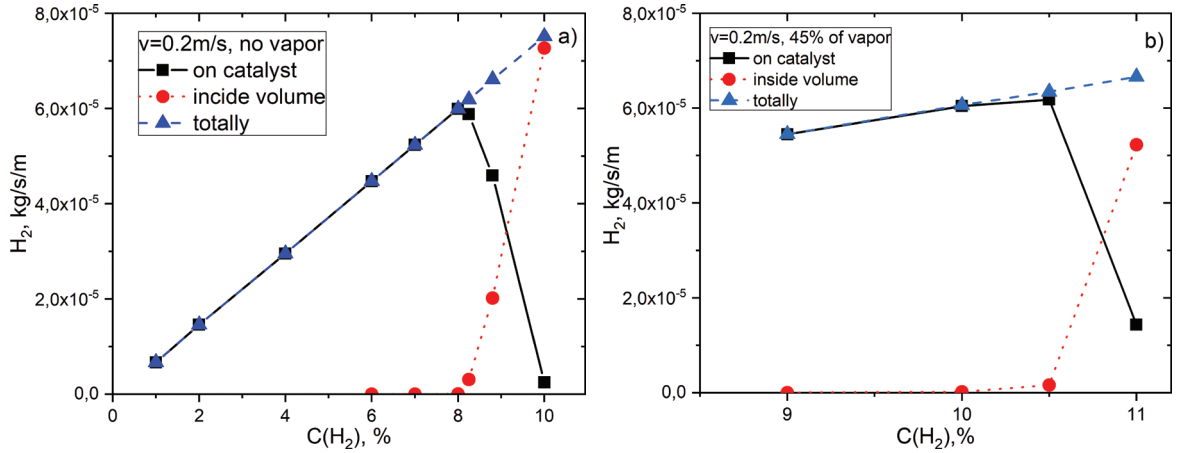

Figure 8. Hydrogen recombination rate as a function of hydrogen concentration, without vapor (**a**) and with a vapor concentration of 45 vol. % (**b**) at the initial time point (inlet flow velocity is 0.2 m/s).

which in turn leads to a decrease in the ignition threshold. Fig. 8 shows the results of calculations at an inlet velocity of the gas mixture of 0.2 m/s. In this case, the initial velocity is lower than it would be with a developed natural circulation for this geometry (about 0.5 m/s).In essence, this mode is the one that inhibits the development of natural circulation. In this case, volumetric ignition of the mixture occurs at high hydrogen concentrations (at about 8 vol. % of hydrogen concentration without steam and at 10.5 vol. % with steam); the recombination rate also drops significantly. The calculations have demonstrated that the higher is the inlet gas mixture flow velocity, the higher is the recombination rate on the catalyst and, therefore, the recombiner efficiency will increase on the whole as well. Thus, for example, the recombination rate is approximately 5 times as high with the flow velocity of 2 m/s as with a velocity of 0.2 m/s (Figs 7, 8).

Conclusions

A uniform approach has been implemented in the STAR CCM+ code environment for analyzing numerically the recombination of hydrogen on a catalytic surface and in a gas phase. A range of practically important results have been obtained for simulation of the PAR operation modes. Essential to the approach is using a detailed mechanism of the hydrogen and oxygen recombination reaction which makes it possible to avoid the adjustment procedure used frequently to determine the single-step reaction parameters for describing the recombiner efficiency. This is a universal approach to determining the efficiency both in conditions of natural circulation and forced circulation in the recombiner region, which is essential at numerical justification of severe accidents with hydrogen release. The RECO-3 and HYSA experiment numerical simulation results are presented which have confirmed that the calculations agree with the available experimental data both qualitatively and quantitatively.

The threshold values of hydrogen concentration for flameless recombination have been calculated and analyzed as a function of external conditions based on the developed CFD approach.

Foundations have been laid for the developed model of the recombiner and vapor-hydrogen-air environment interaction which make it possible to achieve numerically high accuracy and predictability for the computational justification of the hydrogen recombiner operation with any external conditions, including a variety of transients with forced circulation of the vapor-hydrogen-air mixture, this being especially important for numerical simulation of the severe accident progression with hydrogen escape.

References

- Appel C, Mantzaras J, Schaeren R, Bombach R, Inauen A, Kaeppeli B, Hemmerling B, Stampanoni A (2002) An experimental and numerical investigation of homogeneous ignition in catalytically stabilized combustion of hydrogen/air mixtures over platinum, combust. Combustion and Flame 128(4): 340–368. https://doi.org/10.1016/S0010-2180(01)00363-7
- Avdeenkov AV, Sergeev VV, Stepanov AV, Malakhov AA, Koshmanov DY, Soloviev SL, Bessarabov DG (2018) Math hydrogen catalytic recombiner: Engineering model for dynamic full scale calculations. International Journal of Hydrogen Energy 43(52): 23523–23537. https://doi.org/10.1016/j.ijhydene.2018.10.212
- Avdeenkov AV, Kalyakin SG, Soloviev SL, Duong Quang H (2022) On the scalability of the operating capacity of hydrogen recombiners. Nuclear Energy and Technology 8(2): 143–152.
- Bachellerie E, Arnould F, Auglaire M, de Boeck B, Braillard O, Eckardt B, Ferroni F, Moffett R (2003) Generic approach for designing and implementing a passive autocatalytic recombiner PAR-system in nuclear power plant containments. Nuclear Engineering and Design 221: 151–165. https://doi.org/10.1016/S0029-5493(02)00330-8
- Baggemann J, Jahn W, Kelm S, Reinecke EA, Allelein HJ (2017) Numerical study on the influence of different boundary conditions on the efficiency of hydrogen recombiners inside a car garage. International Journal of Hydrogen Energy 42(11): 7608–7616. https://doi.org/10.1016/j.ijhydene.2016.04.084
- Framatome GmbH (2023) Framatome GmbH. https://www.framatome.com/solutionsportfolio/portfolio/product?product=A0640 [accessed May 20, 2023]
- IAEA International Nuclear Information System (2023) IAEA International Nuclear Information System (INIS) IAEA International Nuclear Information System. https://inis.iaea.org/collection/NCLCollectionStore/_Public/33/020/33020098.pdf [accessed May 20, 2023]
- IAEA-TECDOC-1661 (2011) Mitigation of Hydrogen Hazards in Severe Accidents in Nuclear Power Plants. IAEA, Vienna.
- LLC ISPC "Russian Energy Technology" (2023) LLC ISPC "Russian Energy Technology". https://retech.ru/pkrv [accessed May 20, 2023]
- Malakhov A, du Toit H, du Preez SP, Avdeenkov AV, Bessarabov DG (2020) Temperature profile mapping over a catalytic unit of a hydrogen passive autocatalytic recombiner: Experimental and CFD study. Energy Fuels 34(9): 11637–11649. https://doi.org/10.1021/acs.energyfuels.0c01582
- Meynet N, Bentaib A (2012) Numerical study of hydrogen ignition by passive autocatalytic recombiners. Nuclear Technology 178(1): 17–28. https://doi.org/10.13182/NT12-A13544
- Reinecke EA, Bentaib A, Kelm S, Jahn W, Meynet N, Caroli C (2010) Open Issues in the Applicability of Recombiner Experiments and Modelling to Reactor Simulations. Progress in Nuclear Energy 52(1): 136–147. https://doi.org/10.1016/j.pnucene.2009.09.010.
- Reinecke EA, Boehm J, Drinovac P, Struth S, Tragsdorf IM (2005) Modelling of catalytic recombiners: Comparison of REKO DIREKT calculations with REKO-3 experiments, Proceedings of the International Conference "Nuclear Energy for New Europe 2005". Bled, Slovenia, September 5–8, 092.1–092.10
- Reinecke EA, Kelm S, Jahn W, Jäkel C, Allelein HJ (2013) Simulation of the efficiency of hydrogen recombiners as safety devices. International Journal of Hydrogen Energy 38(19): 8117–8124. https://doi.org/10.1016/j.ijhydene.2012.09.093
- San Diego Mechanism web page (2023) Chemical-Kinetic Mechanisms for Combustion Applications. San Diego Mechanism, Mechanical and Aerospace Engineering (Combustion Research), University of California at San Diego. https://web.eng.ucsd.edu/mae/groups/combustion/mechanism.html [accessed May 20, 2023]
- Siemens STAR CCM+ CFD software (2023) Siemens STAR CCM+ CFD software. https://plm.sw.siemens.com/en-US/simcenter/fluids-thermal-simulation/star-ccm/ [accessed May 20, 2023]
- Tarasov OV, Kiselev AE, Filippov AS, Yudina TA, Grigoruk DG, Koshmanov DE, Keller VD, Khristenko EB (2017) Development and verification of a model of RVK-500, -1000 recombiners for modeling the containment shells of NPP with VVER by computational hydrodynamics. Atomic Energy 121(3): 166–172. https://doi.org/10.1007/s10512-017-0178-3